Relaxed Adsorption-flow Coupling Enables Stable COMSOL Modeling of Upscaled Capacitive Deionization

Johan Nordstrand and Joydeep Dutta *

Functional Materials, Applied Physics Department, School of Engineering Sciences, KTH Royal Institute of Technology, AlbaNova universitetscentrum106 91 Stockholm, Sweden
* Correspondence: johanno3@kth.se; joydeep@kth.se; Tel.: +46-8-790-81-42

Introduction

The world population is rapidly expanding and the need for freshwater continues to increase [1,2], making effective desalination technologies [3–11] increasingly important. Capacitive deionization (CDI) [12–14] is an emerging technology in which an electric field stretches between porous electrodes and rapidly extracts salt ions from a centrally passing salt-water stream (Fig. 1). As the technique emerges, the prospect of practically upscaling from lab-scale [15] to pilot plants increasingly grabs many researchers' attention. Now, because material [16–32] and operational [22,33–41] conditions strongly affect CDI performance, spatiotemporal COMSOL simulations are critical for finding the best design principles and operations.

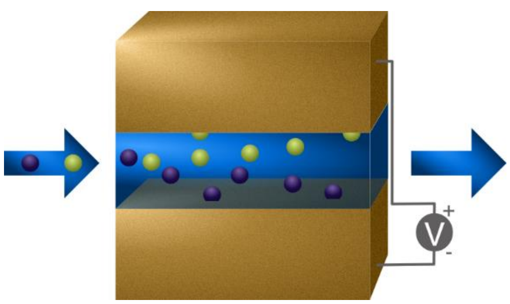

Figure 1. An illustration of a flow-between CDI cell, comprising two porous electrodes separated by a spacer. The applied voltage effectively induces an electric field that strongly pulls the salt ions from the continuously passing water stream.

Various approaches exist for simulating salt-adsorption in porous electrodes through the CDI process, such as the modified Donnan (mD) model [12,13,17,42–44], the dynamic Langmuir (DL) model [45–48], and the circuit-based models [49–51]. While lots of work treats the cell as 0D, some have developed 1D spatiotemporal models along either the flow direction or along the thickness of the electrodes, to capture the transport/diffusion dynamics [16,17,32,42,43,52–54]. Porada et al. made the first attempt at a 2D model by connecting six 1D cells in series [55]. Later, Hemmatifar et al. made the first fully coupled 2D simulation [44]. However, their COMSOL model extensively uses custom interfaces with large systems of coupled differential equations, and they report that the resulting model is "unsteady".

In this work, we present a relaxed-coupling approach that smoothly cuts through the complexities and steadily simulates upscaled CDI with precision. The method uses a 0D Randles circuit as a generator of adsorption in a spatiotemporal ion-transport model in COMSOL. Thus, the Result section will demonstrate that the new model accurately simulates CDI, including upscaled modules, while being able to identify concentration shocks and retaining a low degree of complexity.

Theory

Because this work concerns relaxed adsorption-flow coupling, we will present two separate methods for CDI modeling and then combine them.

Firstly, Fig. 1 shows that the CDI cell is fundamentally a capacitor, and researchers have previously introduced the Randles circuit for describing the charging process (Fig. 2) [51]. This resembles RC charging with a capacitive element C and a resistive element R_1. On top of that, the resistor R_2 describes the leakages through the cell resulting from unwanted electrochemical reactions at the electrode surface.

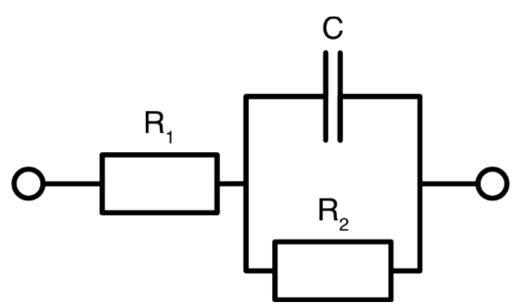

Figure 2. The Randles-circuit representation of a CDI cell. The capacitive element C determines the charge-storage capacity, while the R_2 resistance affects the leakages and R_1 affects the charging rate.

This work's core objective is the simulate salt removal, so notice that the above charging rate relates to the ion-removal rate through the charge efficiency Λ, defined as the fraction between the salt adsorption and charge storage. Previous works have set this to a constant representative value for simplicity [51], and researchers have extensively implemented ion-selective membranes and other methods of getting raising the value to near unity to get as much salt removal as possible from the cell charging.

As the operator implements the Randles model with charge efficiency and becomes aware of the salt removal rate, a transport formulation can finally reveal the actual desalination performance at the outlet. Using a 0D formulation, Equation 1 treats the cell as a flow reactor for salt [56] where the rate at which the cell concentration c is replace with inlet water c_0 depends on the fraction between the flowrate Q and the cell-free volume v_{cell}.

$$\frac{dc}{dt} = -\frac{dc_{ads}}{dt} + \frac{Q}{v_{cell}}(c_0 - c) \tag{1}$$

While researchers have mostly used classic parameter-fitting schemes for CDI, recent research has introduced system-identification methods in MATLAB that lets the operator effectively, reliably, and automatically implement CDI models in a broad range of systems [46,57].

Now that this section has concisely presented the Randles model and a 0D implementation in MATLAB, the next section will rapidly migrate towards the second and crucial implementation method, in COMSOL.

Simulation Methods

While some authors have tried to implement fully coupled 2D CDI models in COMSOL using the modified Donnan (mD), their model comprised extensive custom-built systems of differential equations in COMSOL, and they reported that the resulting model was “unsteady” [44]. Therefore, we will instead use the 0D Randles model as a loosely coupled generator of adsorption.

To start, the COMSOL model [58] fundamentally sets up a CDI cell like the one in Fig. 1, where the background flow ultimately drives the transport processes as solved with the *Brinkman Equations*. All flux through the walls is zero, while the inlet carries a constant flowrate and salt-ion concentration. Thus, the *Transport of Diluted Species in Porous Media* interface simulates the salt-ion transport through the CDI cell. Crucially, the *Reactions* sub-interface defines the rate at which the salt is adsorbed inside the porous electrode. Here, the Randles model generates the loose coupling by separately simulating the adsorption rate and simplifyingly distributing it uniformly throughout the cell. Moving forward, the Methods section will validate that this simplified approach dissolves the complexity barriers while retaining enough detail to solve key CDI simulation questions.

Results and Discussion

The Randles Model

As we presented the bare Randles model you may initially have wondered how well it performs. Consider, therefore, the work by Bouhadana et al. who measured the cumulative charge storage in their CDI system [59]. Figure 3 demonstrates that the Randles simulation excellently matches their experimental data, which means the core model works well for describing the charging rate and leakages.

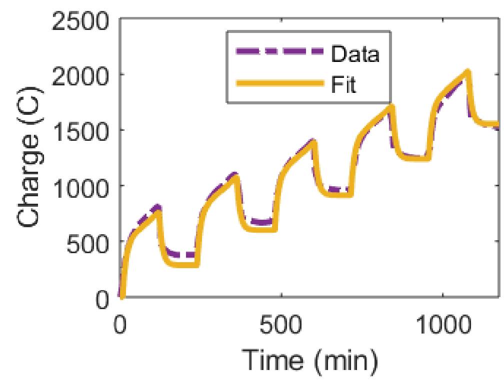

Figure 3. Net charging of a CDI cell, data from Ref. [59]. The net passed charge increases while applying a voltage and decreases when the voltage is removed to release the stored salt ions and regenerate the CDI cell. The difference between the charge passing through the cell during charging and the charge released during discharging constitutes the leakages.

So, what about the actual desalination performance? Consider now Wang et al. who measured the effluent concentration in their membrane-CDI system [60]. Because the system had a membrane, we simplifyingly assumed ideal charge efficiency and leakage, and then again fitted the Randles circuit. The agreement between model and experiment is again excellent, thus the results soundly validate the approach for simulating both current (Fig. 4a) and concentration (Fig. 4b). Wang et al. also operated the system in a constant-current mode; that is, the voltage is ramped up so that the current is always the same. By using the model fit form Figure 4ab and the known ramped-up voltage, the model now accurately predicts the new output ion concentration (Fig. 4c). This means the 0D Randles model works well for both fitting and predicting CDI systems under these reasonable conditions.

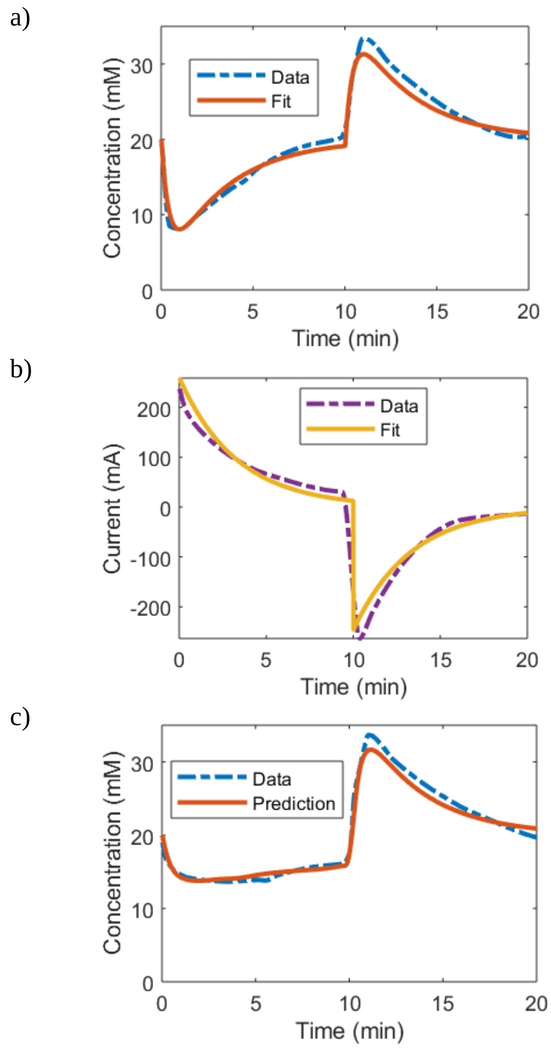

Figure 4. Cell-effluent concentration during the charging and discharging of the CDI cell. **(a, b)** A system-identification method in MATLAB fitted the Randles-circuit model to concentration and current data from Ref. [60]. **(c)** Using the fitting in (a) and the known applied voltage, the model accurately predicts the effluent concentration during a constant-current operation with the same device [60].

The Relaxed-coupling approach

So, if the 0D model works well under normal conditions, when is it at all relevant to complicate simulations by using a 2D model? Hemmatifar et al. found that a major strength of using a fully spatiotemporal approach is that the operator can discover localized ion-depleted regions where the adsorption is extremely slow because there are hardly any ions to adsorb [44]. These regions could easily arise if the operator raises the voltage to speed up the desalination process but the flowrate brings in new ions too slowly, or a lacking cell construction prevents diffusion at the rate required to sustain the desired adsorption rate.

As we begin to use the 2D COMSOL model, first recall that the validated 0D-Randles model accurately simulates the total adsorption and current. Thus, we will now further demonstrate that uniformly inserting known adsorption and current trends into a transport model in COMSOL can yield effective performance predictions while allowing the operator to identify concentration shocks. Figs. 5ab demonstrate that this approach yields solid results relative to experimental data under normal conditions. In fact, the quality is similar to that of the fully coupled model by Hemmatifar et al. [44], and validates the relaxed-coupling approach to stable 2D simulations. Moving on, Fig. 5c further shows the crucial point that the relaxed-coupling approach works for identifying concentration shocks too since the spatial resolution finds the concentration-shocked areas.

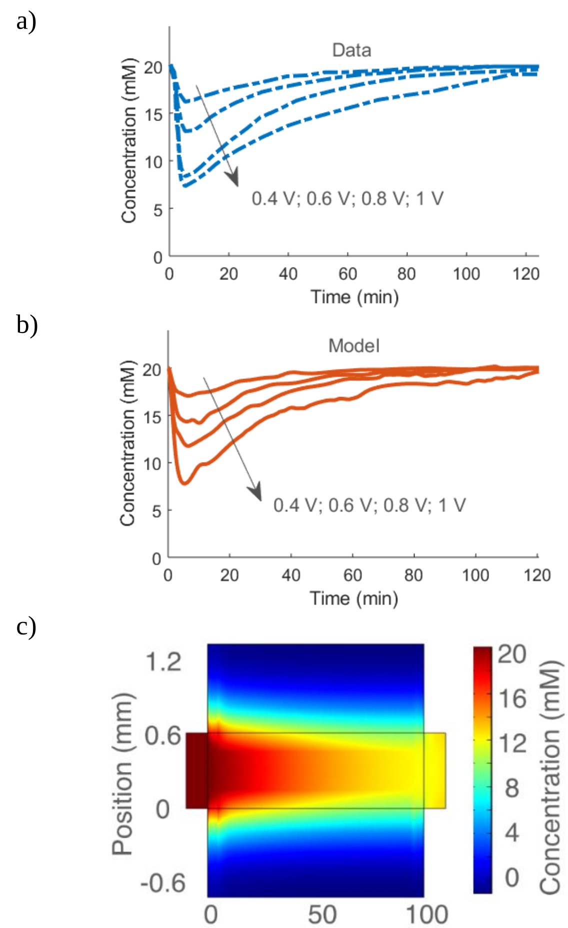

Figure 5. (a) Effluent ion concentration for a range of applied voltages, data from Ref. [44]. **(b)** COMSOL effectively and tractably predicts the effluent concentration by using prior fitting data from Fig. 5 in Ref. [44] to separately determine the uniform reaction rate for the *Reactions* interface. **(c)** For the highest voltages, the simulated interior concentration can reach zero, strongly indicating that the ion-starvation conditions are hampering the desalination process.

A downside with the bare Randles model is that it does not incorporate the impact large variations in concentration can have on the adsorption rate. This means the quantitative accuracy under such conditions could be lower, and some researchers have expanded the bare model to account for this [61]. While we could have implemented such an extension, the crucial point to note is that the present relaxed-coupling approach qualitatively finds the starved areas, which is enough to know that the cell should be operated or constructed differently.

To summarize, if the construction/operation is terrible the model finds how to solve it, and if the construction/operation is feasibly good the model quantitatively predicts the desalination performance.

Upscaling

Thus far, this work has demonstrated that the relaxed-coupling approach predicts desalination performance and finds concentration shocks with substantially less complexity than the fully 2D method. So, having this relax model now raises the question: is there a deeper inherent value to reducing complexity apart from making the model more accessible? Fundamentally, the risk of having core models that are unsteady even in small systems is that they might not feasibly allow computations for expanded and intricate cell construction.

Following this reasoning, let us investigate how the relaxed coupling approach applies to larger cell modules. Fig. 6 shows the structure we used to simulate a stacked two-cell system. The model again simplifies the computations, here by assuming that the two-cell system removes twice as much salt as the single-cell system. For this simulation, the operator could either scale the Randles model to size or use the simplest operation and double the experimentally measured performance for the single-cell system, thus thoroughly eliminating separate simulations. The point is that the core model or experiment can generate a simulation for a modular structure without adding complexity.

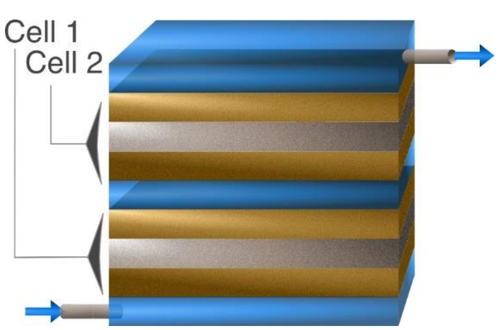

Figure 6. A schematic showing two serially coupled CDI cells. The water enters from the bottom and passes both cells before exiting at the top.

A benefit of upscaling simulation is that they can investigate the advantages of various modular connections. Figs. 7ab show simulations for two-cell modules connection in series and parallel, respectively. Thus, COMSOL reports that the desalination performance is equal (Fig. 7c), but the pressure drop for the parallel system is just a quarter of the pressure drop for the serial system, which means that the parallel system is highly preferable in CDI constructions.

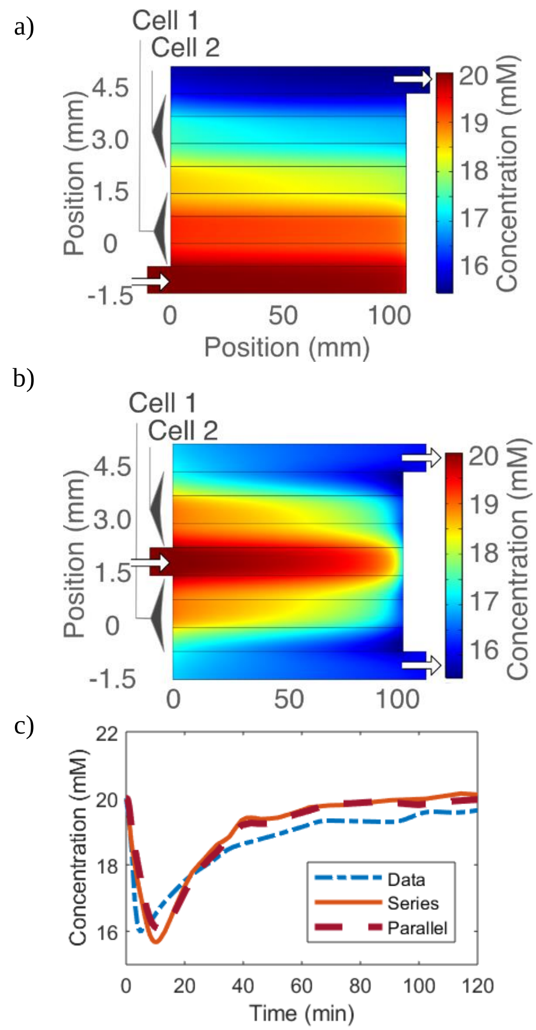

Figure 7. (a, b) Snapshots of desalination simulations at the time of lowest effluent concentration for a two-cell system stacked in series and parallel, respectively. **(c)** This graph compares the experiment cell-effluent concentration at 0.4 V (from Fig. 5a) to the corresponding simulated effluent concentration for serial and parallel modules with doubled size and flowrate.

Conclusions

Developing new and existing desalination technologies is crucial for meeting the increasing global demand for drinkable water, and many researchers are increasingly devoting attention to the promising and emerging CDI technique. As it emerges, effective, and reliable simulation methods for upscaled CDI modules are becoming increasingly important.

Because previous work has found the state-of-the-art models for 2D spatiotemporal CDI modeling in COMSOL to be "unsteady" [44], this word firmly introduced a novel relaxed-coupling approach. Therein, a separate 0D-Randles circuit simulates the adsorption rate onto the porous electrode in the CDI cell, a rate that subsequently enters as a reaction rate in COMSOL's *Transport of Diluted Species in Porous Media* interface. Experimental data reveal that this method accurately fit and predicts various CDI operation, and effectively identifies concentration shocks that hamper the desalination performance.

A key point in this work is that the presented relaxed-coupling approach fundamentally dissolves the computational complexity barrier which allows the model to solidly simulate upscaled systems. As a proof-of-concept, we simulated a two-cell stack and demonstrated that a parallel connection yields the same desalination performance as a serial system with a quarter of the pressure drop.

Finally, we express our hope that this work sparks researchers' interest and propel the use of the relaxed-coupling approach for upscaled capacitive deionization. We also encourage proponents of fully coupled approaches to extensively develop tractable implementations in COMSOL that will allow researchers to accurately simulate detailed CDI phenomena also in upscaled modules.

References

(1) WWAP (United Nations World Water Assessment Programme)/UN-Water. *United Nations World Water Dev. Rep. 2018 Nature-Based Solut. Water* **2018**.

(2) Eltawil, M. A.; Zhengming, Z.; Yuan, L. A Review of Renewable Energy Technologies Integrated with Desalination Systems. *Renew. Sustain. Energy Rev.* **2009**, *13* (9), 2245–2262. https://doi.org/10.1016/j.rser.2009.06.011.

(3) Ghaffour, N.; Missimer, T. M.; Amy, G. L. Technical Review and Evaluation of the Economics of Water Desalination : Current and Future Challenges for Better Water Supply Sustainability. *DES* **2015**, *309* (2013), 197–207. https://doi.org/10.1016/j.desal.2012.10.015.

(4) Alghoul, M. A.; Poovanaesvaran, P.; Sopian, K.; Sulaiman, M. Y. Review of Brackish Water Reverse Osmosis (BWRO) System Designs. *Renew. Sustain. Energy Rev.* **2009**, *13*, 2661–2667. https://doi.org/10.1016/j.rser.2009.03.013.

(5) Fahmida, P.; Sultana, A. Desalination Technologies for Developing Countries : A Review. *J. Sci. Res.* **2018**, *10* (January), 77–97.

(6) Lee, K. P.; Arnot, T. C.; Mattia, D. A Review of Reverse Osmosis Membrane Materials for Desalination — Development to Date and Future Potential. *J. Memb. Sci.* **2011**, *370* (1–2), 1–22. https://doi.org/10.1016/j.memsci.2010.12.036.

(7) Greenlee, L. F.; Lawler, D. F.; Freeman, B. D.; Marrot, B.; Moulin, P.; Ce, P. Reverse Osmosis Desalination : Water Sources , Technology , and Today ' s Challenges. *Water Res.* **2009**, *43* (9), 2317–2348. https://doi.org/10.1016/j.watres.2009.03.010.

(8) Strathmann, H. Electrodialysis , a Mature Technology with a Multitude of New Applications. *DES* **2010**, *264* (3), 268–288. https://doi.org/10.1016/j.desal.2010.04.069.

(9) Mcginnis, R. L.; Elimelech, M. Energy Requirements of Ammonia – Carbon Dioxide Forward Osmosis Desalination. *Desalination* **2007**, *207*, 370–382. https://doi.org/10.1016/j.desal.2006.08.012.

(10) Kim, T.; Gorski, C. A.; Logan, B. E. Low Energy Desalination Using Battery Electrode Deionization. *Environ. Sci. Technol. Lett.* **2017**, *4* (10), 444–449. https://doi.org/10.1021/acs.estlett.7b00392.

(11) Rommerskirchen, A.; Ohs, B.; Arturo, K.; Femmer, R. Modeling Continuous Flow-Electrode Capacitive Deionization Processes with Ion-Exchange Membranes. *J. Memb. Sci.* **2018**, *546* (October 2017), 188–196. https://doi.org/10.1016/j.memsci.2017.10.026.

(12) Porada, S.; Zhao, R.; Van Der Wal, A.; Presser, V.; Biesheuvel, P. M. Review on the Science and Technology of Water Desalination by Capacitive Deionization. *Prog. Mater. Sci.* **2013**, *58* (8), 1388–1442. https://doi.org/10.1016/j.pmatsci.2013.03.005.

(13) Suss, M. E.; Porada, S.; Sun, X.; Biesheuvel, P. M.; Yoon, J.; Presser, V. Water Desalination via Capacitive Deionization: What Is It and What Can We Expect from It? *Energy Environ. Sci.* **2015**, *8* (8), 2296–2319. https://doi.org/10.1039/C5EE00519A.

(14) Anderson, M. A.; Cudero, A. L.; Palma, J. Capacitive Deionization as an Electrochemical Means of Saving Energy and Delivering Clean Water. Comparison to Present Desalination Practices: Will It Compete? *Electrochim. Acta* **2010**, *55* (12), 3845–3856. https://doi.org/10.1016/j.electacta.2010.02.012.

(15) Tang, W.; Liang, J.; He, D.; Gong, J.; Tang, L.; Liu, Z.; Wang, D.; Zeng, G. Various Cell Architectures of Capacitive Deionization: Recent Advances and Future Trends. *Water Res.* **2019**, *150*, 225–251. https://doi.org/10.1016/j.watres.2018.11.064.

(16) Mutha, H. K.; Cho, H. J.; Hashempour, M.; Wardle, B. L.; Thompson, C. V.; Wang, E. N. Salt Rejection in Flow-between Capacitive Deionization Devices. *Desalination* **2018**, *437* (January), 154–163. https://doi.org/10.1016/j.desal.2018.03.008.

(17) Guyes, E. N.; Shocron, A. N.; Simanovski, A.; Biesheuvel, P. M.; Suss, M. E. A One-Dimensional Model for Water Desalination by Flow-through Electrode Capacitive Deionization. *Desalination* **2017**, *415*, 8–13. https://doi.org/10.1016/j.desal.2017.03.013.

(18) Porada, S.; Bryjak, M.; Van Der Wal, A.; Biesheuvel, P. M. Effect of Electrode Thickness Variation on Operation of Capacitive Deionization. *Electrochim. Acta* **2012**, *75*, 148–156. https://doi.org/10.1016/j.electacta.2012.04.083.

(19) Li, H.; Zou, L.; Pan, L.; Sun, Z. Using Graphene Nano-Flakes as Electrodes to Remove Ferric Ions by Capacitive Deionization. *Sep. Purif. Technol.* **2010**, *75* (1), 8–14. https://doi.org/10.1016/j.seppur.2010.07.003.

(20) Wang, G.; Ling, Y.; Qian, F.; Yang, X.; Liu, X. X.; Li, Y. Enhanced Capacitance in Partially Exfoliated Multi-Walled Carbon Nanotubes. *J. Power Sources* **2011**, *196* (11), 5209–5214. https://doi.org/10.1016/j.jpowsour.2011.02.019.

(21) Długołęcki, P.; van der Wal, A. Energy Recovery in Membrane Capacitive Deionization. *Environ. Sci. Technol.* **2013**, *47*, 4904–4910. https://doi.org/10.1021/es3053202.

(22) Tang, W.; He, D.; Zhang, C.; Waite, T. D. Optimization of Sulfate Removal from Brackish Water by Membrane Capacitive Deionization (MCDI). *Water Res.* **2017**, *121*, 302–310. https://doi.org/10.1016/J.WATRES.2017.05.046.
(23) Choi, J.-H.; Yoon, D.-J. The Maximum Allowable Charge for Operating Membrane Capacitive Deionization without Electrode Reactions. *Sep. Purif. Technol.* **2019**, *215*, 125–133. https://doi.org/10.1016/j.seppur.2019.01.003.
(24) Zhao, X.; Wei, H.; Zhao, H.; Wang, Y.; Tang, N. Electrode Materials for Capacitive Deionization: A Review. *J. Electroanal. Chem.* **2020**, *873*, 114416. https://doi.org/https://doi.org/10.1016/j.jelechem.2020.114416.
(25) Qu, Y.; Campbell, P. G.; Hemmatifar, A.; Knipe, J. M.; Loeb, C. K.; Reidy, J. J.; Hubert, M. A.; Stadermann, M.; Santiago, J. G. Charging and Transport Dynamics of a Flow-Through Electrode Capacitive Deionization System. *J. Phys. Chem. B* **2018**, *122* (1), 240–249. https://doi.org/10.1021/acs.jpcb.7b09168.
(26) Laxman, K.; Husain, A.; Nasser, A.; Al, M.; Dutta, J. Tailoring the Pressure Drop and Fluid Distribution of a Capacitive Deionization Device. *Desalination* **2019**, *449* (July 2018), 111–117. https://doi.org/10.1016/j.desal.2018.10.021.
(27) Xu, X.; Li, J.; Li, Y.; Ni, B.; Liu, X.; Pan, L. Selection of Carbon Electrode Materials. In *Interface Science and Technology*; Elsevier, Ed.; Elsevier Ltd., 2018; Vol. 24, pp 65–83. https://doi.org/10.1016/B978-0-12-811370-7.00004-8.
(28) Laxman, K.; Tay, M.; Myint, Z.; Bourdoucen, H.; Dutta, J. Enhancement in Ion Adsorption Rate and Desalination Efficiency in a Capacitive Deionization Cell through Improved Electric Field Distribution Using Electrodes Composed of Activated Carbon Cloth Coated with Zinc Oxide Nanorods. *Appl. Mater. interfaces* **2014**, *6*, 10113−10120. https://doi.org/10.1021/am501041t.
(29) Laxman, K.; Myint, M. T. Z.; Khan, R.; Pervez, T.; Dutta, J. Improved Desalination by Zinc Oxide Nanorod Induced Electric Field Enhancement in Capacitive Deionization of Brackish Water. *Desalination* **2015**, *359*, 64–70. https://doi.org/10.1016/j.desal.2014.12.029.
(30) Laxman, K.; Myint, M. T. Z.; Khan, R.; Pervez, T.; Dutta, J. Effect of a Semiconductor Dielectric Coating on the Salt Adsorption Capacity of a Porous Electrode in a Capacitive Deionization Cell. *Electrochim. Acta* **2015**, *166*, 329–337. https://doi.org/10.1016/j.electacta.2015.03.049.
(31) Suss, M. E.; Baumann, T. F.; Worsley, M. A.; Rose, K. A.; Jaramillo, T. F.; Stadermann, M.; Santiago, J. G. Impedance-Based Study of Capacitive Porous Carbon Electrodes with Hierarchical and Bimodal Porosity. *J. Power Sources* **2013**, *241*, 266–273. https://doi.org/10.1016/j.jpowsour.2013.03.178.
(32) Suss, M. E.; Baumann, T. F.; Bourcier, W. L.; Spadaccini, C. M.; Rose, K. A.; Santiago, J. G.; Stadermann, M. Capacitive Desalination with Flow-through Electrodes. *Energy Environ. Sci.* **2012**, *5* (11), 9511. https://doi.org/10.1039/c2ee21498a.
(33) Demirer, O. N.; Naylor, R. M.; Rios Perez, C. A.; Wilkes, E.; Hidrovo, C. Energetic Performance Optimization of a Capacitive Deionization System Operating with Transient Cycles and Brackish Water. *Desalination* **2013**, *314*, 130–138. https://doi.org/10.1016/j.desal.2013.01.014.
(34) Biesheuvel, P. M.; Porada, S.; Levi, M.; Bazant, M. Z. Attractive Forces in Microporous Carbon Electrodes for Capacitive Deionization. *J. Solid State Electrochem.* **2014**, *18* (5), 1365–1376. https://doi.org/10.1007/s10008-014-2383-5.
(35) Zhao, R.; Soestbergen, M. Van; Rijnaarts, H. H. M.; Wal, A. Van Der; Bazant, M. Z.; Biesheuvel, P. M. Time-Dependent Ion Selectivity in Capacitive Charging of Porous Electrodes. *J. Colloid Interface Sci.* **2012**, *384* (1), 38–44. https://doi.org/10.1016/j.jcis.2012.06.022.
(36) Seo, S.; Jeon, H.; Kwang, J.; Kim, G.; Park, D.; Nojima, H.; Lee, J.; Moon, S. Investigation on Removal of Hardness Ions by Capacitive Deionization (CDI) for Water Softening Applications. *Water Res.* **2010**, *44* (7), 2267–2275. https://doi.org/10.1016/j.watres.2009.10.020.
(37) Tang, W.; Kovalsky, P.; Cao, B.; Waite, T. D. Investigation of Fluoride Removal from Low-Salinity Groundwater by Single-Pass Constant-Voltage Capacitive Deionization. *Water Res.* **2016**, *99*, 112–121. https://doi.org/10.1016/j.watres.2016.04.047.
(38) Fan, C. S.; Tseng, S. C.; Li, K. C.; Hou, C. H. Electro-Removal of Arsenic(III) and Arsenic(V) from Aqueous Solutions by Capacitive Deionization. *J. Hazard. Mater.* **2016**, *312*, 208–215. https://doi.org/10.1016/j.jhazmat.2016.03.055.
(39) Tang, W.; Kovalsky, P.; He, D.; Waite, T. D. Fluoride and Nitrate Removal from Brackish Groundwaters by Batch-Mode Capacitive Deionization. *Water Res.* **2015**, *84*, 342–349. https://doi.org/10.1016/j.watres.2015.08.012.
(40) Hou, C.; Huang, Z.-Y. A Comparative Study of Electrosorption Selectivity of Ions by Activated Carbon Electrodes in Capacitive Deionization. *Desalination* **2013**, *369*, 46–50. https://doi.org/10.1016/j.desal.2015.04.022.
(41) Wang, C.; Song, H.; Zhang, Q.; Wang, B.; Li, A. Parameter Optimization Based on Capacitive Deionization for Highly Efficient Desalination of Domestic Wastewater Biotreated Effluent and the Fouled Electrode Regeneration. *Desalination* **2015**, *365*, 407–415. https://doi.org/10.1016/j.desal.2015.03.025.
(42) Biesheuvel, P. M.; Fu, Y.; Bazant, M. Z. Diffuse Charge and Faradaic Reactions in Porous Electrodes. *Phys. Rev. E* **2011**, *83* (6). https://doi.org/10.1103/PhysRevE.83.061507.
(43) Suss, M. E.; Biesheuvel, P. M.; Baumann, T. F.; Stadermann, M.; Santiago, J. G. In Situ Spatially and Temporally Resolved Measurements of Salt Concentration between Charging Porous Electrodes for Desalination by Capacitive Deionization. *Environ. Sci. Technol.* **2014**, *48* (3), 2008–2015. https://doi.org/10.1021/es403682n.
(44) Hemmatifar, A.; Stadermann, M.; Santiago, J. G. Two-Dimensional Porous Electrode Model for Capacitive Deionization. *J. Phys. Chem. C* **2015**, *119* (44), 24681–24694. https://doi.org/10.1021/acs.jpcc.5b05847.
(45) Nordstrand, J.; Dutta, J. Dynamic Langmuir Model: A Simpler Approach to Modeling Capacitive Deionization. *J. Phys. Chem. C* **2019**, *123* (26), 16479–16485. https://doi.org/10.1021/acs.jpcc.9b04198.
(46) Nordstrand, J.; Laxman, K.; Myint, M. T. Z.; Dutta, J. An Easy-to-Use Tool for Modeling the Dynamics of Capacitive Deionization. *J. Phys. Chem. A* **2019**, *123* (30), 6628–6634. https://doi.org/10.1021/acs.jpca.9b05503.
(47) Nordstrand, J.; Dutta, J. Simplified Prediction of Ion noRemoval in Capacitive Deionization of Multi-Ion Solutions. *Langmuir* **2020**, *0* (January). https://doi.org/10.1021/acs.langmuir.9b03571.
(48) Nordstrand, J.; Dutta, J. Predicting and Enhancing the Ion Selectivity in Multi-Ion Capacitive Deionization. *Langmuir* **2020**. https://doi.org/10.1021/acs.langmuir.0c00982.
(49) Qu, Y.; Campbell, P. G.; Gu, L.; Knipe, J. M.; Dzenitis, E.; Santiago, J. G.; Stadermann, M. Energy Consumption Analysis of Constant Voltage and Constant Current Operations in Capacitive Deionization. *Desalination* **2016**, *400*, 18–24. https://doi.org/10.1016/j.desal.2016.09.014.

(50) Qu, Y.; Baumann, T. F.; Santiago, J. G.; Stadermann, M. Characterization of Resistances of a Capacitive Deionization System. *Environ. Sci. Technol.* **2015**, *49* (16), 9699–9706. https://doi.org/10.1021/acs.est.5b02542.
(51) Qin, M.; Deshmukh, A.; Epsztein, R.; Patel, S. K. Comparison of Energy Consumption in Desalination by Capacitive Deionization and Reverse Osmosis. *Desalination* **2019**, *455*, 100–114. https://doi.org/10.1016/j.desal.2019.01.003.
(52) Biesheuvel, P. M.; Bazant, M. Z. Nonlinear Dynamics of Capacitive Charging and Desalination by Porous Electrodes. *Phys. Rev. E - Stat. Nonlinear, Soft Matter Phys.* **2010**, *81* (3), 1–12. https://doi.org/10.1103/PhysRevE.81.031502.
(53) Biesheuvel, P. M.; Zhao, R.; Porada, S.; van der Wal, A. Theory of Membrane Capacitive Deionization Including the Effect of the Electrode Pore Space. *Journal of Colloid and Interface Science*. 2011, pp 239–248. https://doi.org/10.1016/j.jcis.2011.04.049.
(54) Perez, C. A. R.; Demirer, O. N.; Clifton, R. L.; Naylor, R. M.; Hidrovo, C. H. Macro Analysis of the Electro-Adsorption Process in Low Concentration NaCl Solutions for Water Desalination Applications. *J. Electrochem. Soc.* **2013**, *160* (3), E13–E21. https://doi.org/10.1149/2.025303jes.
(55) Porada, S.; Borchardt, L.; Oschatz, M.; Bryjak, M.; Atchison, J. S.; Keesman, K. J.; Kaskel, S.; Biesheuvel, P. M.; Presser, V. Direct Prediction of the Desalination Performance of Porous Carbon Electrodes for Capacitive Deionization. *Energy Environ. Sci.* **2013**, *6* (12), 3700–3712. https://doi.org/10.1039/c3ee42209g.
(56) Hawks, S. A.; Knipe, J. M.; Campbell, P. G.; Loeb, C. K.; Hubert, M. A.; Santiago, J. G.; Stadermann, M. Quantifying the Flow Efficiency in Constant-Current Capacitive Deionization. *Water Res.* **2018**, *129*, 327–336. https://doi.org/10.1016/j.watres.2017.11.025.
(57) Nordstrand, J.; Dutta, J. Basis and Prospects of Combining Electroadsorption Modeling Approaches for Capacitive Deionization. *Physics (College. Park. Md).* **2020**, *2* (2), 309–324. https://doi.org/10.3390/physics2020016.
(58) COMSOL. Porous Media Flow Module https://www.comsol.com/porous-media-flow-module (accessed Apr 13, 2020).
(59) Bouhadana, Y.; Ben-Tzion, M.; Soffer, A.; Aurbach, D. A Control System for Operating and Investigating Reactors: The Demonstration of Parasitic Reactions in the Water Desalination by Capacitive de-Ionization. *Desalination* **2011**, *268* (1–3), 253–261. https://doi.org/10.1016/j.desal.2010.10.037.
(60) Wang, L.; Lin, S. Membrane Capacitive Deionization with Constant Current vs Constant Voltage Charging: Which Is Better? *Environ. Sci. Technol.* **2018**, *52* (7), 4051–4060. https://doi.org/10.1021/acs.est.7b06064.
(61) Ramachandran, A.; Oyarzun, D. I.; Hawks, S. A.; Campbell, P. G.; Stadermann, M.; Santiago, J. G. Comments on "Comparison of Energy Consumption in Desalination by Capacitive Deionization and Reverse Osmosis." *Desalination* **2019**, *461* (March), 30–36. https://doi.org/10.1016/j.desal.2019.03.010.

Acknowledgements

The authors would like to thank the Swedish research council (Diary No. 2018-05387) and J. Gust. Richert stiftelse (Diary No. 2020-00584) for funding the work.